Synthetic small molecule analogues of the immunomodulatory *Acanthocheilonema viteae* product ES-62 promote metabolic homeostasis during obesity in a mouse model

Felicity E. Lumb[a*], Jenny Crowe[b*], James Doonan[a], Colin J. Suckling[c], Colin Selman[d], Margaret M. Harnett[b] and William Harnett[a†]

[a]Strathclyde Institute of Pharmacy and Biomedical Sciences, University of Strathclyde, Glasgow G4 0RE, UK

[b]Institute of Infection, Immunity and Inflammation, University of Glasgow, Glasgow G12 8TA, UK

[c]Department of Pure and Applied Chemistry, University of Strathclyde, Glasgow, G1 1XL, UK

[d]Glasgow Ageing Research Network (GARNER), Institute of Biodiversity, Animal Health and Comparative Medicine, University of Glasgow, Glasgow, G12 8QQ, UK

*Joint first authors

†Corresponding author: Prof. William Harnett, Strathclyde Institute of Pharmacy and Biomedical Sciences, 161 Cathedral Street, Glasgow G4 0RE, UK; phone: 0044-141-548-3725; e.mail: w.harnett@strath.ac.uk

Abstract

One of the most rapidly increasing human public health problems is obesity, whose sequelae like type-2 diabetes, represent continuously worsening, life-long conditions. Over the last 15 years, data have begun to emerge from human and more frequently, mouse studies, that support the idea that parasitic worm infection can protect against this condition. We have therefore investigated the potential of two synthetic small molecule analogues (SMAs) of the anti-inflammatory *Acanthocheilonema viteae* product ES-62, to protect against metabolic dysfunction in a C57BL/6J mouse model of high calorie-induced obesity. We found weekly subcutaneous administration of the SMAs in combination (1 μg of each), starting one week before continuous exposure to high calorie diet (HCD), decreased fasting glucose levels and reversed the impaired glucose clearance observed in male mice, when measured at approximately 7 and 13 weeks after exposure to HCD. Fasting glucose levels were also improved in male mice fed a HCD for some 38 weeks when given SMA-treatment 13 weeks after the start of HCD, indicating an SMA-therapeutic potential. For the most part, protective effects were not observed in female mice. SMA treatment also conferred protection against each of reduced ileum villus length and liver fibrosis, but more prominently in female mice. Previous studies in mice indicate that protection against metabolic dysfunction is usually associated with polarisation of the immune system towards a type-2/anti-inflammatory direction but our attempts to correlate improved metabolic parameters with such changes were unsuccessful. Further analysis will therefore be required to define mechanism of action. Nevertheless, overall our data clearly show the potential of the drug-like SMAs as a preventative or treatment for metabolic dysregulation associated with obesity.

Keywords: ES-62; glucose; helminth; metabolic syndrome; nematode; type 2 diabetes

1. Introduction

The world is experiencing an obesity epidemic: over a third of the world's adult population are defined as obese or overweight and this number is on the rise [1]. Obesity greatly increases the risk of developing enduring disease morbidities such as insulin resistance, type-2 diabetes, metabolic syndrome, depression, cardiovascular disease and cancer, as these pathologies are promoted by the chronic, low-grade inflammation commonly associated with this condition. Such inflammation reflects that the stress on adipose tissue skews the immune system towards a type-1 response characterised by M1-like macrophages, neutrophils and pro-inflammatory cytokines, resulting in a vicious cycle involving the release of free fatty acids and pro-inflammatory markers such as TNF-α and IL-6 that drives dysregulation of immunometabolic networks and ultimately insulin resistance [2-4]. By contrast, a predominantly type-2 inflammatory response involving eosinophils and alternatively activated (M2-like) macrophages (AAMs) has been shown to be important for the maintenance of healthy adipose tissue [4-6].

Parasitic helminths represent a group of organisms that generally induce a strong, type-2 immune response in their hosts, that is characterised by increases in eosinophils, AAMs and mast cells and the production of cytokines such as IL-4 and IL-5. In addition, this response is often accompanied by a regulatory component which is associated for example, with the production of IL-10 and expansion of regulatory T and B cells (reviewed in [7]). This regulatory response is likely to contribute to parasitic worms being able to exist within their hosts for years, if not decades, without causing pathology. At the same time, the generation of an anti-inflammatory environment by parasitic worms has been considered to result in beneficial spill-over effects. Thus, a number of studies have demonstrated the ability of helminth infections, or molecules that helminths release (excretory-secretory products; E-S),

to protect against, or ameliorate, both allergic diseases like asthma and autoimmune diseases such as rheumatoid arthritis, type-1 diabetes and inflammatory bowel disease (reviewed in [8-10]). Furthermore, the observation that systemic inflammation plays a key role in the development of insulin resistance in obesity has led researchers to investigate, using mouse models, whether helminths can improve glucose tolerance and insulin sensitivity in obesity. Thus, for example, infection with *Nippostrongylus brasiliensis* [5], *Schistosoma mansoni [11]*, *Heligomosoides polygyrus* [12] and *Litomoisoides sigmondontis* [13, 14] has been proven to improve insulin sensitivity in diet-induced mouse models of obesity. Similar effects were observed with treatment with helminth products. For example, Bhargava *et al* [15] demonstrated that LNFPIII, a component of *S. mansoni*, significantly improved glucose clearance and decreased extent of hepatosteatosis in obese mice. Additionally, it was found that schistosome [11] and *Litomosoides* [14] adult worm antigen extracts had the same protective effect as live worm infection. Helminth products have also been shown to play a disease-preventing role in murine models of atherosclerosis: for example, schistosome soluble egg antigen extract (SEA) treatment resulted in a 44% reduction in atherosclerotic plaque size in a cholesterol-induced murine model of atherosclerosis [16].

ES-62, a phosphorylcholine (PC) containing glycoprotein secreted by the filarial nematode *Acanthocheilonema viteae*, has been shown to have protective effects in a number of autoimmune and allergic mouse models such as collagen-induced arthritis (CIA; [17]), the MRL/*Lpr* model of systemic lupus erythematosus (SLE; [18]) and the ovalbumin-induced airway hypersensitivity model of asthma ([19, 20]). Additionally, ES-62 reduces aortic plaques by almost 60% in the *Gld*.ApoE$^{-/-}$ mouse model of accelerated atherosclerosis, a cardiovascular condition often observed in SLE patients [21]. Although these results suggest that ES-62 could have widespread therapeutic potential, it constitutes a large, “foreign” and

hence likely immunogenic molecule that in addition, cannot be generated in active recombinant form [22] due to incomplete knowledge of the biosynthetic pathway responsible for addition of its active moiety, PC (reviewed by [23]). Thus, in case these factors should hamper its development towards the clinic, we have generated a library of PC-based small molecule analogues. Two of these SMAs, 11a and 12, have been shown to have similar protective effects to ES-62 in the mouse models of arthritis [24, 25], asthma [26, 27] and SLE [28]. The primary mechanism of action of the SMAs is the direct targeting of MyD88 for degradation that results in consequent downregulation of inflammation [29]. As MyD88 also interacts with the master metabolic sensor and highly conserved lifespan determinant, mTOR to integrate chronic inflammation, metabolic deregulation, oxidative stress and mitochondrial dysfunction [30-32], we wished to investigate whether the SMAs could positively impact on insulin resistance and adipose and liver tissue dysregulation in a diet-induced model of obesity.

2. Methods

2.1 Animals

All the experimental procedures were approved by and conducted according to the Animal Welfare and Ethical Review Body at the University of Glasgow and UK Home Office Regulations and License PPL 60/4504. C57BL/6J mice (male and female; Charles River, UK) were divided into 3 groups: chow-fed-PBS-treated, HCD-fed PBS control, and HCD-fed SMA treated. The mice were injected once a week subcutaneously with PBS (control) or a combination of SMAs 11a plus 12b (1μg of each) from 9 weeks old. All mice had *ad libitum* access to water and a chow diet (CRM-P; SDS, UK; Oil, 3.36%; Protein 18.35%; Fibre, 4.23%: Sugar 3.9%; Atwater fuel energy from Oil, 9.08%; Protein, 22.03%: Carbohydrate, 68.9%) plus 150 ppm Fenbendazole until 10 weeks of age. The HCD groups were then switched onto a western diet (HCD; Fat, 21.4%; Protein, 17.5; Fibre, 3.5%; Sucrose 33%; Atwater fuel energy from Fat, 42%; Protein, 15%: Carbohydrate, 43%; SDS, UK) plus 150 ppm Fenbendazole. Mice were monitored daily and weighed weekly. Cohorts of mice were sacrificed at day (d)160 (n=4-6/group) and at d 340 (n=8/group) days of age and tissues were harvested. At d340 there was an additional group: HCD-fed SMA therapeutic (n=8; male and female). These mice were switched to a HCD at 10 weeks old but did not received SMA (11a+12b) injections until 23 weeks (d160) and again culled at d340.

At sacrifice, the mesenteric lymph nodes (MLN) and retroperitoneal (dorsal fat pad directly behind the kidneys and attached to the peritoneum) adipose depots were recovered and prepared for flow cytometry analysis. In addition, liver, adipose, ileum and colon tissues were fixed in 10% neutral buffered formalin, and embedded in paraffin, or flash frozen in OCT and stored at -80°C for future analysis.

2.2. Histology and Image Analysis

Retroperitoneal adipose tissue was frozen in OCT and cryosectioned (ThermoScientific, UK) at 8-15 μm thickness at -30°C. Liver and gut tissues were embedded in paraffin and sectioned at 6 μm. All tissues were stained with haematoxylin and eosin (H&E), and liver tissue sections were Gömöri's Trichrome stained using previously described methods [33]. Brightfield images were captured using an EVOS FI Auto. Liver fat droplet deposition was calculated as the percentage "white area" (using a set threshold) relative to the total area of tissue in FOV in Volocity software, and collagen deposition was quantified as the percentage staining in FOV using ColourDeconvolution plugin and ImageJ software. Individual adipocyte area and adipocyte numbers in FOV of adipose tissue were calculated using Adipocount software (CSBIO). In the ileum and colon, the villi length (from crypt to tip) and crypt depth was measured using ImageJ software in 3 separate FOVs for each mouse and averaged.

2.3 Flow Cytometry

Retroperitoneal adipose tissue was digested in 1 mg/ml Collagenase type II (Sigma, UK) for 45 minutes at 37°C with gentle agitation and then passed through 100 μM filter to generate the stromal vascular fraction (SVF). Red blood cells in MLN and SVF cell suspensions were lysed (eBioscience, UK); cells were then washed in FACS buffer (2.5% BSA; 0.5 mM EDTA, in PBS) and then incubated with Fc block (Biolegend, UK) prior to staining with the relevant antibodies/streptavidin conjugates (all BioLegend, UK unless stated otherwise). In adipose tissues, eosinophils were characterised as SiglecF+ (PE: Catalogue number 552126 BD Bioscience, UK), and constitutive IL-10 expression was identified using anti-IL-10 antibody (APC: catalogue number 505009). B regulatory cells in the MLN were identified by CD19 (AF700: Catalogue number 115527), B220 (PerCP: catalogue number 103235) and IL-

10 (PE: Catalogue number 505007) expression [34]. Fixable viability stain (eFluor™450: Catalogue number 65-0863-14; eBioscience, UK) was used to select for live cells. Data was acquired using a BD LSRII flow cytometer and populations were gated using isotype and fluorescence minus one (FMO) controls using FlowJo, LLC analysis software (Tree Star/ BD) as described previously [20, 34].

2.4. Glucose tolerance testing

Mice were fasted overnight and their blood glucose level (nmol/L) was measured using an accu-check performa (Roche, UK) or OneTouch Ultra (Lifescan, UK) glucometer. Mice were then injected intraperitoneally with 20% glucose solution (2 g glucose/kg body weight) and their blood glucose levels were measured at 15, 30, 60 and 120 minutes-post injection, with blood samples obtained by caudal vein venesection.

2.5. qRT-PCR

Adipose tissue was lysed in QIAzol prior to mRNA extraction using the DNA away RNA extraction kit (NBS Biologicals, UK) and mRNA was transcribed into cDNA using the High Capacity cDNA Reverse Transcriptase kit (Applied Biosystems, Life Technology, UK). Changes in gene expression were measured using KiCqStart® qPCR ready mix (Sigma-Aldrich) and KiCqStart™ Primers on an Applied Biosystems Quant Studio 7. Data were normalized to the housekeeping gene β-actin to obtain the ΔCT values that were used to calculate the 2^-ΔCT. Primer sequences were: β-actin (forward-GATGTATGAAGGCTTTGGTC, reverse-TGTGCACTTTTATTGGTCTC), IL-4 (forward-CTGGATTCATCGATAAGCTG, reverse- TTTGCATGATGCTCTTTAGG), IL-5 (forward-

CCCTACTCATAAAAATCACCAG, reverse-TTGGAATAGCATTTCCACAG), TNF-α (forward- CTATGTCTCAGCCTCTTCTC, reverse-CATTTGGGAACTTCTCATCC) TripBr2 (forward-CCACTTGTAACACACTCTTC, reverse-TCAACATTAGCAACACAGTC).

2.6. Statistical Analysis

All data was analysed using GraphPad Prism 6 or 8 software using two-way ANOVA (GTT), one-Way ANOVA (with Fishers LSD post-test for parametric data) or student's t-tests. Significance is denoted by *$p < 0.05$, **$p < 0.01$ and ***$p < 0.001$.

3. Results

3.1. SMA treatment reduces HCD-induced increased adipose tissue mass in male mice

We investigated whether combination treatment with SMAs 11a plus 12b could have a positive impact on metabolic health in mice fed a high calorie diet (HCD), when compared to such mice given PBS and also PBS-treated chow-fed animals. Consumption of the HCD resulted in a significant increase in the body mass of both male and female mice by 160 days of age (Figure 1a), compared to their counterparts fed a standard chow diet. SMA, versus PBS, treatment had no significant effect on HCD-induced increased body mass of either male or female mice at 160 days of age (Figure 1a) and this was also the case at day 340 (results not shown). However, in male but not female mice, SMA administration slowed the HCD-induced increase in retroperitoneal adipose depots (as a proportion of body mass) as evidenced by the reduction in the levels determined at 160 (Figure 1b), but not 340 (results not shown) days of age. Consistent with this finding, histological analysis revealed that SMA treatment similarly slowed the HCD-increase in retroperitoneal adipocyte size, as corroborated by quantitative analysis of the HCD-decrease in adipocyte numbers detected per field of view and also the HCD-enlargement of adipocyte area (albeit this last readout didn't reach statistical significance) at day 160 (but not 340) in male but not female HCD-mice (Figure 1c-e and results not shown).

3.2. SMA-treatment does not alter immunological parameters in adipose tissue

In an attempt to understand the mechanism underlying the SMAs' protective effects against HCD-induced changes in retroperitoneal adipose tissue in male mice at day 160, we measured a range of immunological parameters. Unlike the protection against metabolic changes induced by living parasitic worms described in previous studies [5, 35], SMA-

protection in male mice did not appear to reflect a repolarisation of T-helper type-1/2 (Th-1/2) inflammation as we did not observe any induction of eosinophils (Figure 2a) or increased production of mRNA for the Th-2 cytokines IL-4 and IL-5 (Figure 2b & c) when comparing PBS- versus SMA-treated, HCD-fed animals. Also, no effect on levels of anti-inflammatory IL-10^{+} cells (Figure 2d), or expression of the pro-inflammatory cytokine TNF-*a* (Figure 2e) was observed. Furthermore, we assessed expression of mRNA for the master regulator of adiposity, TripBr2 [36], but as with the immunological parameters, we did not see any SMA-induced effect (Figure 2f).

3.3. SMA-treatment improves fasting glucose levels and impaired glucose clearance in male HCD-fed mice

We next investigated the effect of HCD on the ability of mice to metabolise blood glucose, as retroperitoneal adipose tissue impacts on glucose tolerance with enhanced mass being associated with dysregulation of tissue function. We show that after 6-7 weeks of HCD (day 116), fasted male mice had an impaired ability to clear blood-glucose compared to chow mice following administration of a bolus of glucose (glucose tolerance test; GTT): strikingly, this was converted back to chow-levels by treatment with SMAs 11a plus 12b (Figure 3a). Treatment with the SMAs also significantly lowered the fasting blood glucose levels of male mice at this time point (Figure 3b). Furthermore, the protective effect of SMA treatment on glucose clearance was still evident at 160 days of age, although somewhat diminished (Figure 3c). Likewise, there remained some evidence of a protective effect on fasting glucose levels, as PBS-treated HCD-fed mice but not SMA-treated HCD-fed mice, showed significant glucose intolerance relative to chow-fed animals at this time point (Figure 3d). In contrast, the SMAs did not significantly modulate glucose clearance, or reduce fasting glucose levels, in HCD-fed female mice at either time point (Figure 3e & f and results not shown).

240 **3.4. SMA treatment can improve some aspects of HCD-induced liver and gut pathology**

241 Chronic feeding with HCD can have a significant impact on liver function: increased free
242 fatty acids - a result of insulin resistance - are deposited in the liver. This can cause
243 inflammation and tissue disruption leading to the development of steatosis and fibrosis [3, 4].
244 Given that the SMAs ameliorated HCD-induced glucose intolerance in male mice (Figure 3)
245 we measured various parameters associated with liver pathology. Histological analysis
246 revealed that male mice in particular, when fed a HCD, did indeed exhibit steatosis by day
247 160 (Figure 4a) but the SMAs did not protect against this in either sex at either day 160 or
248 340 (Figure 4b & c and results not shown). Fibrosis, as indicated by collagen deposition, was
249 also detected in the livers of both male and female mice fed a HCD by d160. For this
250 pathology, the levels were similar between the two sexes and unlike for steatosis, the SMAs
251 significantly protected against this in female HCD-fed animals at both time points (Figure 4d
252 & e and results not shown).
253
254 Continuous exposure to a HCD can also seriously impact on gut health and, consistent with
255 this, we found histopathological evidence of ileal damage at d160 in both sexes (Figure 5a).
256 Male PBS-treated HCD-fed animals revealed a significant decrease in villi length when
257 compared to chow-fed animals, but this decrease was absent in the SMA-treated HCD-fed
258 mice (Figure 5b). The decrease in villi length witnessed with female PBS-treated HCD-fed
259 mice did not reach statistical significance, however, villi length in SMA-treated HCD-fed
260 mice was significantly increased relative to the PBS-treated, HCD-fed mice and was
261 comparable to that of chow-fed animals (Figure 5c). No HCD-effects were observed in the
262 colon at the same time-point (results not shown). Interestingly, we noted that damage to the
263 ileum in both sexes was associated with a significant HCD-induced decrease in mesenteric

lymph node (MLN) regulatory B cells (Bregs; $CD19^{+}B220^{+}IL\text{-}10^{+}$). However, SMA-treatment did not significantly rebalance this (Figure 5d & e).

3.5. SMA-treatment is protective when administered therapeutically to HCD-fed obese mice

We next investigated whether the combination of SMAs 11a and 12b had any protective effect in a therapeutic situation, namely when their administration was delayed until ~13 weeks after the start of the HCD (day 160) and assessment undertaken following a further 180 days of HCD feeding and treatment with SMAs. As observed at day 160 and day 340 with prophylactic SMA treatment, there was no significant effect of the treatment on body mass of either male or female mice (Figure 6a). However, unlike with the prophylactic model at day 160 (but not 340), therapeutic SMA administration from day 160 had no effect on the size of the retroperitoneal adipose depots in male (and also female) HCD-fed animals at 340 days of age (Figure 6b). This was supported by histopathological analysis, which showed that SMAs (when administered either prophylactically or therapeutically) had no significant effect on either the number or average adipocyte area of adipocytes (per field of view) in retroperitoneal adipose tissue when compared to HCD-PBS mice at d340 (Figure 6c-e, and results not shown). Moreover, as shown by the GTT-time course, by day 340 glucose tolerance had undergone a remodelling process in male HCD-fed mice such that it is removed more rapidly from the circulation relative to the younger cohort (Figure 7a), possibly due to the increased capacity to take-up glucose provided by their enlarged visceral adipose tissues [37]. Interestingly, treatment with 11a plus 12b (either prophylactically or therapeutically) significantly reversed this remodelling such that the glucose clearance in SMA-treated HCD-fed male mice more resembled that of chow-fed mice (Figure 7a and results not shown). Nevertheless, whilst fasting glucose levels were increased in the PBS-treated HCD-fed male

animals relative to chow-fed mice, this was significantly reduced by therapeutic SMA-treatment (Figure 7b). Collectively these data suggest that the SMAs support "chow-like" glucose handling throughout d116-d340 in male mice, despite the chronic exposure to HCD from d70. Female mice do not experience the HCD-induced glucose metabolism remodelling observed with male mice at the 340-day time-point as shown by the GTT and hence HCD-fed mice still show increased persistence in the bloodstream relative to chow-fed animals (Figure 7c). However, unlike the situation at day 116 and 160 with prophylactic treatment, SMA-treated HCD-fed female mice show a significant improvement in glucose clearance following therapeutic treatment with SMAs (Figure 7c) although perhaps surprisingly this was not accompanied by a modulation of fasting glucose levels (Figure 7d). Also, we did not observe any improved glucose clearance with female mice at day 340 in the prophylactic model (results not shown).

We also examined liver fibrosis following therapeutic administration of the SMAs: as with the prophylactic models (d160, Figure 4 and d340, data not shown), we observed a statistically significant protective effect against the HCD-induced collagen deposition but not steatosis in female but not male mice (Figure 8 and results not shown). In addition, unlike at day 160, we observed HCD-induced colon damage in male (but not female; results not shown) mice as revealed by a significant decrease in crypt depth between chow-fed and PBS-treated HCD-fed mice. However, this significance was absent between chow-fed and HCD-fed animals treated with the SMAs either prophylactically (data not shown) or therapeutically at d340 (Figure 9a & b). Focusing on mechanism of action again, we also measured MLN Bregs at this time point: as observed earlier, these were reduced by HCD but SMA-treatment (either prophylactically or therapeutically) did not reverse this (Figure 9 and results not shown).

4. Discussion

Emerging evidence suggests that parasitic worm infection can have positive effects on metabolic regulation. This has led to the idea that the worms might be exploited as a treatment against obesity, a rapidly increasing global health problem that can result in a number of serious health conditions such as type-2 diabetes, for which current treatment approaches result in unwanted side effects. This evidence is largely derived from studies employing mouse models of obesity, in which parasitic worms or their molecules have been shown to improve glucose tolerance [5, 11, 13, 14]. Moreover, it has also been shown that humans infected with gastrointestinal nematodes develop increased insulin resistance following treatment with an anthelmintic [38]. We now provide further support for the protective effects of worms when employing two synthetic small molecule analogues (SMAs) of ES-62, a major secreted protein of *A. viteae* that is immunomodulatory by virtue of multiple covalently attached phosphorylcholine (PC) residues [reviewed in [8] and [39]], in a C57BL/6J mouse model of obesity. We employed the SMA combination because although both compounds are protective in mouse models of diseases associated with aberrant inflammation like rheumatoid arthritis, they show subtle differences in immunomodulatory mechanism of action [24, 25]. Like the parent molecule, the SMAs appear to be safe as evidenced by our administration of them to mice on a weekly basis for 9-10 months with no adverse effects noted during careful monitoring in this study and consistent with this, we had previously witnessed no toxic effects *in vitro* when assessing staining of macrophages with 7-AAD or worsening of inflammatory disease *in vivo* in acute (1-2 months) mouse models [24, 25]. As the SMAs are also cost-effective and straightforward to produce, they represent an attractive starting point for novel drug development.

As expected, exposure to a HCD, resulted in a significant increase in body mass in both male and female mice. SMA-treatment did not protect against this increase. However, there were some indications that the molecules were having more-subtle beneficial effects, in that HCD-induced changes occurring in visceral adipose tissue were somewhat reduced in male mice exposed to the SMA- versus PBS-treatment at day 160. Previous studies using live worm infection have provided mixed results when examining effects on whole body and adipose tissue mass [11-14] but this may in part reflect worm species differences and/or variation in experimental design. The reduction in adipose tissue mass that we witnessed was associated with male mice only and was no longer present by day 340. Considering the known association between increased body mass and decreased glucose homeostasis, we went on to examine whether the SMAs would affect glucose handling. HCD treatment resulted in impaired glucose tolerance and this was observed at both day 116 and 160 in the male mice. Data from the GTT analysis showed that SMA-treatment significantly protected against impaired HCD-induced glucose intolerance and fasting plasma glucose levels were also lower in SMA-treated mice at both ages. These effects were more apparent at the earlier time point initially leading us to consider that with respect to glucose clearance, the SMAs may eventually struggle to be effective as metabolic dysfunction progresses. However, remarkably by the time the HCD-fed mice have reached 340 days of age, they can remove glucose from the circulation even more effectively than chow-fed mice and perhaps somewhat ironically the SMA-treatment actually converts the GTT values back towards the chow-fed phenotype. This remodelling effect has been described previously [37]: it is considered to be due to increased glucose uptake via enlarged visceral adipose tissues and may help protect the body against further obesity-induced damage. Presumably it is less obvious in SMA-treated mice because overall, they develop less visceral adipose tissue (we only examined retroperitoneal adipose tissue) or at least the increase is delayed, as shown in the present study for

retroperitoneal tissue. Interestingly, overall the SMAs appear to be more effective than ES-62 in dealing with rising blood glucose levels although we did not test the early day 116 timepoint with the parent molecule [40]. We did not observe any protective effect of the SMAs on glucose clearance in female mice in the current study but such animals appear to show somewhat less impairment of this in response to HCD than males.

We also determined the effects of SMA-treatment on a number of other HCD-induced pathological alterations – liver steatosis and fibrosis, gut ileum and colon damage. We found no protection against steatosis but reduced fibrosis in both sexes, although this was only statistically significant in female mice. These data for both steatosis and fibrosis mirror what we observed when treating HCD-fed mice with ES-62 [40], although with the parent molecule, protection against fibrosis in the male mice also reached statistical significance. Nevertheless, returning to steatosis, *H. polygyrus* can markedly improve this in diabetic mice [12, 41], indicating different effects from the ES-62-SMAs. Regarding gut damage, we found evidence of HCD-induced ileum damage (reduced villus length at d160) that was protected against by SMA treatment, particularly in female animals. Again, these gut data largely mirror what we have observed with ES-62 [40].

The protection observed with the SMAs in what effectively is a prophylactic model, supports their use as a potential preventive medicine against the health conditions associated with obesity. However, another more likely option would be to employ the compounds as a therapeutic and with this in mind, we investigated whether the SMAs still offered any protective effects when their administration was delayed until approximately 13 weeks after the start of the HCD (day 160). With this therapeutic administration, we did not observe any effect on retroperitoneal adipose tissue. The SMA treatment did however result in glucose

clearance showing a chow-like rather than HCD-like phenotype and this was also true of fasting glucose levels. Interestingly, in the therapeutic model at day 340 when examining female mice, which do not undergo the remodelling of glucose handling observed in their male counterparts, for the first time we found some evidence of protection against impaired glucose clearance. However, there was no improvement in fasting glucose levels in these animals. Female mice undergoing the prophylactic regimen did not reveal any protection at the same day 340-time point. Thus overall, the female situation with respect to glucose homeostasis is rather less clear-cut than the male. Interestingly however, as observed with prophylactic SMA administration, therapeutically-treated female mice appear to suffer less liver fibrosis. Overall, it is encouraging that both sexes appear to respond to SMA treatment in a therapeutic setting in some manner, raising the possibility that SMA-based drugs might be considered for use in this manner in male and female humans. Nevertheless, on the whole, the differences between the two sexes that we observe are intriguing in that they suggest both that male and female mice may suffer differing degrees of particular obesity-induced pathologies and also, register differences in the ability of the SMAs to prevent the pathologies. Possibly at least some of the variation we have observed with respect to both factors could relate to sex-specific differences in hormone levels and it could therefore be interesting to investigate the effects of hormonal intervention in our system. We have also observed sex-specific responses to ES-62 treatment with this model [40] but as far as we are aware, this has not been reported with other defined helminth-derived molecules that are protective in mouse models of inflammatory diseases.

To date, we have obtained a significant amount of mechanistic data when employing the SMAs in mouse models of allergy and autoimmunity. Thus, for example, we have found that like ES-62, the SMAs reduce the production of cytokines that are important in driving the

414 inflammatory response [24, 25, 27], reset the effector: regulatory B cell balance to the non-
415 inflammatory situation [27, 28] and promote degradation of the TLR adaptor MyD88 [29]. In
416 the present study, we undertook mechanistic analysis based on previously published papers
417 outlining how parasitic worms helped maintain glucose homeostasis. Thus, for example, Wu
418 *et al*. [5] showed that homeostasis in adipose tissue was dependent on AAMs induced by IL-4
419 released from eosinophils and thus, that infection with *N. brasiliensis*, by increasing levels of
420 adipose tissue eosinophils, could protect against obesity-induced impaired homeostasis.
421 Likewise, protection offered by *L. sigmodontis* is associated with increased eosinophils and
422 AAMs in adipose tissue [14]. However, when investigating retroperitoneal adipose tissue
423 from male animals at the day 160 time point we did not witness any change in levels of
424 eosinophils or mRNA for IL-4 or the related cytokine that plays multiple roles in eosinophil
425 biology, IL-5 in adipose tissue. Likewise, taking into account the known increased
426 inflammatory nature of adipose tissue from HCD-fed mice we measured levels of the anti-
427 inflammatory IL-10-producing cells and the pro-inflammatory cytokine TNF-α, but SMA-
428 treatment did not increase the former or reduce the latter. One possible explanation for these
429 results is that we may be past the point where SMA-protection is optimal in the model, as
430 when examining the GTT data the SMAs appeared to be more effective at day 116 than day
431 160. Thus, examining day 116 tissue for immune cell and cytokine profiles during this earlier
432 time point may be warranted. Nevertheless, in spite of detecting some reductions in
433 inflammatory- and increases in anti-inflammatory-markers in the ES-62 study referred to
434 earlier [40], these changes did not appear to be the key factors that improved healthspan or
435 lifespan in ageing animals. Rather a more convincing case – supported by a machine learning
436 approach – was provided by metabolic changes and improved gut health/reduced gut
437 dysbiosis. Furthermore, although an increase in adipose tissue IL-10 was observed with
438 protective *H. polygyrus* infection [12, 41], Berbudi *et al.* [14] did not observe a role for this

cytokine when observing protective effects with *L. sigmodontis.* In any case, the protective effects we observe on retroperitoneal adipose tissue could be related to other non-immunological factors. We thus examined levels of mRNA for TRIP-Br2, a transcription factor that regulates fat lipolysis: TRIP-Br2's expression is elevated in visceral fat in obese humans and in addition, knockout mice are resistant to obesity-induced insulin resistance [36]. However, we did not observe any reduction in TRIP-Br2 expression. Nevertheless, there are a number of other genes involved in glucose homeostasis that might be worth examining: in particular, these might include glucose transporters (considered to be drug targets in Type-2 diabetes) such as GLUT2 and GLUT4, whose expression is modified by *H. polygyrus* [12] and *L. sigmodontis* respectively [14].

We also observed that the HCD-induced gut damage was associated with a decrease in MLN Bregs but that the SMAs could not reverse this. Although we have previously observed that the SMAs can overturn alterations in the effector: regulatory B cell balance, our work with ES-62 indicates that changes in Bregs are dynamic and may only occur during certain checkpoints throughout the disease model [27, 40]. In any case, a further study should investigate whether we are actually witnessing downregulation of MyD88 in immune system and tissue effector cells when the SMAs are employed in the model, given the uniformity of this event with difference cell types exposed to ES-62/SMAs to date, including effector B cells [18, 24, 25, 27]. We did not examine levels of T regs ($CD25^+FoxP3^+$) or Tr1 (IL-10^+CD4^+) cells as our experience from a number of mouse models of allergic [27] and autoimmune [18] diseases is that ES-62 does not induce such cells. In any case, Tregs appeared to play no role in *L. sigmodontis*-protection against impaired glucose clearance although increased Foxp3 expression was observed in MLN cells during protective *H. polygyrus* infection [12, 41].

464

465 A final factor, which needs to be considered when investigating the mechanism of action of
466 the SMAs in ameliorating glucose intolerance is the microbiome. It has recently been shown
467 [42] that *Strongyloides venzuelensis* improves insulin sensitivity and signalling in mice by
468 impacting on the composition of the gut microbiome. Although this is associated with
469 induction of an anti-inflammatory environment in adipose tissue, which we have not
470 witnessed with the SMAs in the current study, we have recently found ES-62 to also
471 modulate the composition of the mouse gut microbiome during both HCD-accelerated ageing
472 [40] and collagen-induced arthritis [34]. We now plan to establish whether a similar situation
473 occurs with SMA-treatment.

474

475 5**. Acknowledgements**

476 The study was funded by linked awards to MMH and CS (BB/M029727/1) and WH
477 (BB/M029662/1) from the Biotechnology and Biological Sciences Research Council.

Figure Legends

Figure 1: SMAs reduce adipocyte hypertrophy in male HCD-fed mice. Data in panels a and b are presented as the values of individual mice. (a) PBS- and SMAs-treated HCD-male (Blue; ***p<0.001) and -female (Red; *p<0.05) mice exhibited substantially higher Body Mass (BM) than their aged-matched chow (also PBS-treated) control groups. In addition, the male mice were significantly heavier at cull than their female counterparts (chow, **p<0.01, PBS, ***p<0.001). (b) Analysis of retroperitoneal fat (% BM) of chow, PBS- or SMAs-treated HCD mice at cull, where *p<0.05 for male HCD-SMAs versus HCD-PBS mice. Representative images (scale bar 100 μm) of retroperitoneal fat from male chow- and HCD-mice stained with H & E (c) and resultant quantitative analysis of adipocyte number (d) and size (e) where d160 data are presented as the mean values (derived from n=3 replicate analyses) for individual mice where, *p < 0.05 for HCD-PBS versus HCD-SMAs mice. The p value for male HCD-PBS versus HCD-SMAs is shown on the figure in panel e. For Chow mice, n=2 due to the very limited amounts of retroperitoneal tissue recovered from these lean male mice. Statistical analysis is by one-way ANOVA or student's t-test.

Figure 2: SMAs do not modulate the Th1/Th2 balance in retroperitoneal adipose tissue in male HCD-fed mice. The levels of SiglecF$^+$ eosinophils (% live SVF cells) from retroperitoneal adipose tissue of PBS- and SMAs-treated mice are presented for individual animals in each cohort (a). qRT-PCR analysis of IL-4 (b) and IL-5 (c) mRNA expression in retroperitoneal fat from male PBS- and SMAs-treated mice where data are expressed as $2^{\Delta CT}$ values of individual mice and where the values for each mouse are means of n=3 replicate analyses. (d) The levels of IL-10$^+$ cells (% live SVF cells) in retroperitoneal fat in male PBS- and SMAs-treated mice in the d160 cohorts are shown. qRT-PCR analysis of TNFα (e) and TripBr2 (f) mRNA expression in retroperitoneal fat from male PBS- and SMAs-treated mice where data are expressed as 2^ΔCT values of individual mice and where the values for each mouse are means of n=3 replicate analyses.

Figure 3: SMAs modulate glucose handling in male HCD-fed mice. Glucose tolerance tests (GTT) were undertaken at d116 (a - male, e - female) and one week before the d160 cull (c - male, f- female) with fasting glucose measured at d116 (b) and at d160 cull (d) in male mice. GTT data are presented as mean values ± SEM of individual male (d116, chow n=8; PBS n=6; SMAs n=8; d160 cull, chow n=4; PBS n=6; SMAs n=6) and female (d116, chow n=6; PBS n=5; SMAs n=8; d160 cull, chow n=4; PBS n=6; SMAs n=5) mice at each time point, where *p<0.05 and ***p<0.001 for HCD-PBS versus HCD-SMAs by two-way ANOVA (a, c) and *p< 0.05 for HCD-PBS versus HCD-SMAs or chow by one-way ANOVA (b, d).

Figure 4: SMAs reduce liver fibrosis. (a) Representative images (scale bar 100 μm) of liver from male and female mice stained with Gömöri's Trichrome: quantitative analysis of fat (b & c) and collagen deposition (d & e) is presented as mean (of triplicate analyses) values of individual male (b & d) and female (c & e) mice. Significant difference between the HCD-PBS and HCD-SMAs cohorts is shown where *p < 0.05 by one-way ANOVA.

Figure 5: SMAs ameliorate gut pathology. (a) Representative images (scale bar 500 μm) of ileum tissue from male and female chow- and HCD- (PBS- or SMAs-treated) d160 mice stained with H & E (upper panels) and Gömöri's Trichrome (lower panels). Quantitative analysis of ileum villus length (b, c) are shown. Data are presented as the mean values for individual mice, where the values for each mouse are means derived from n=3 replicate

analyses and where *p<0.05 for HCD-PBS versus Chow (b) and HCD-SMAs (c). (d, e) MLN IL-10$^+$ Bregs (B220$^+$CD19$^+$IL-10$^+$; % live cells) are presented as the values for individual male (d) and female (e) mice and where **p<0.05 and ***p<0.001 for chow versus HCD-PBS (and female HCD-SMAs) mice by one-way ANOVA or student's t-test.

Figure 6: Therapeutic treatment with SMAs from d160 (SMAsT) does not reduce adipocyte hypertrophy in HCD-fed mice at d340. (a) HCD-male (Blue; ***p<0.001) and -female (Red; **p<0.01) mice exhibited substantially higher Body Mass (BM) than their aged-matched chow control groups. In addition, male mice were significantly heavier at cull than their female counterparts (chow, ***p<0.001, PBS, ***p<0.001, where data are from individual mice). (b) Analysis of retroperitoneal fat (% BM) of chow, PBS- or SMAsT-treated HCD mice at cull where data are presented as the values of individual mice, and **p<0.01 for HCD-PBS versus chow mice. Representative images (scale bar 100 μm) of retroperitoneal fat (c) from female chow- and HCD- (PBS- or SMAsT-treated) mice stained with H & E and resultant quantitative analysis of adipocyte size where data are presented as the mean values (derived from n=3 replicate analyses) for individual mice where, *p < 0.05 and ***p<0.001 for HCD-PBS versus chow mice by one-way ANOVA.

Figure 7: Therapeutic treatment with SMAs modulates glucose handling in HCD-fed mice. Glucose tolerance tests (GTT) were undertaken one week before the d340 cull (a, c) with fasting glucose measured at cull (b & d). GTT data are presented as mean values ± SEM of individual male (n=8 all cohorts) and female (chow n=6; PBS n=7; SMAsT n=8) mice at each time point, where *p<0.05, **p<0.01 and ***p<0.001 for HCD-PBS versus HCD-SMAsT by two-way ANOVA (GTT) or one-way ANOVA (fasting glucose).

Figure 8: Therapeutic treatment with SMAs reduces liver fibrosis in female HCD-fed mice at d340. (a) Representative images (scale bar 100 μm) of liver from male and female mice stained with Gömöri's Trichrome: quantitative analysis of collagen deposition (b & c) is presented as mean (of triplicate analyses) values of individual male (b) and female (c) mice. Significant difference between the HCD-PBS and HCD-SMAsT cohorts is shown where *p < 0.05 by one-way ANOVA.

Figure 9: Therapeutic treatment with SMAs reduces colon damage in male HCD-fed mice at d340. (a) Representative images (scale bar 500 μm) of colon tissue from male chow- and HCD- (PBS- or SMAsT-treated) mice at d340 stained with H & E (upper panels) and Gömöri's Trichrome (lower panels) and quantitative analysis of crypt depth (b) are shown. Data are presented as the mean values of individual male mice, where the values for each mouse are means derived from n=3 replicate analyses and *p<0.05 for HCD-PBS versus Chow. (c) MLN IL-10$^+$ Bregs (B220$^+$CD19$^+$IL-10$^+$; % live cells) are presented as the values for individual male mice, where *p<0.05 for HCD-PBS versus chow mice by one-way ANOVA.

References

[1] A. Hruby, F.B. Hu, The Epidemiology of Obesity: A Big Picture, PharmacoEconomics 33(7) (2015) 673-89.

[2] J.M. Olefsky, C.K. Glass, Macrophages, inflammation, and insulin resistance, Annu Rev Physiol 72 (2010) 219-46.

[3] M.S. Ellulu, I. Patimah, H. Khaza'ai, A. Rahmat, Y. Abed, Obesity and inflammation: the linking mechanism and the complications, Arch Med Sci 13(4) (2017) 851-863.

[4] H.L. Caslin, A.H. Hasty, Extrinsic and Intrinsic Immunometabolism Converge: Perspectives on Future Research and Therapeutic Development for Obesity, Curr Obes Rep 8(3) (2019) 210-219.

[5] D. Wu, A.B. Molofsky, H.E. Liang, R.R. Ricardo-Gonzalez, H.A. Jouihan, J.K. Bando, A. Chawla, R.M. Locksley, Eosinophils sustain adipose alternatively activated macrophages associated with glucose homeostasis, Science (New York, N.Y) 332(6026) (2011) 243-7.

[6] P.F. Weller, L.A. Spencer, Functions of tissue-resident eosinophils, Nature Reviews Immunology 17(12) (2017) 746-760.

[7] R.M. Maizels, Parasitic helminth infections and the control of human allergic and autoimmune disorders, Clin Microbiol Infect 22(6) (2016) 481-6.

[8] M.M. Harnett, W. Harnett, Can Parasitic Worms Cure the Modern World's Ills?, Trends in Parasitology 33(9) (2017) 694-705.

[9] T.B. Smallwood, P.R. Giacomin, A. Loukas, J.P. Mulvenna, R.J. Clark, J.J. Miles, Helminth Immunomodulation in Autoimmune Disease, Frontiers in Immunology 8 (2017) 453.

[10] Z. Wu, L. Wang, Y. Tang, X. Sun, Parasite-Derived Proteins for the Treatment of Allergies and Autoimmune Diseases, Frontiers in Microbiology 8 (2017) 2164.

[11] L. Hussaarts, N. Garcia-Tardon, L. van Beek, M.M. Heemskerk, S. Haeberlein, G.C. van der Zon, A. Ozir-Fazalalikhan, J.F. Berbee, K. Willems van Dijk, V. van Harmelen, M. Yazdanbakhsh, B. Guigas, Chronic helminth infection and helminth-derived egg antigens promote adipose tissue M2 macrophages and improve insulin sensitivity in obese mice, FASEB J 29(7) (2015) 3027-39.

[12] M. Morimoto, N. Azuma, H. Kadowaki, T. Abe, Y. Suto, Regulation of type 2 diabetes by helminth-induced Th2 immune response, J Vet Med Sci 78(12) (2017) 1855-1864.

[13] A. Berbudi, J. Ajendra, A.P. Wardani, A. Hoerauf, M.P. Hubner, Parasitic helminths and their beneficial impact on type 1 and type 2 diabetes, Diabetes/Metabolism Research and Reviews 32(3) (2016) 238-50.

[14] A. Berbudi, J. Surendar, J. Ajendra, F. Gondorf, D. Schmidt, A.L. Neumann, A.P. Wardani, L.E. Layland, L.S. Hoffmann, A. Pfeifer, A. Hoerauf, M.P. Hubner, Filarial Infection or Antigen Administration Improves Glucose Tolerance in Diet-Induced Obese Mice, J Innate Immun 8(6) (2016).

[15] P. Bhargava, C. Li, K.J. Stanya, D. Jacobi, L. Dai, S. Liu, M.R. Gangl, D.A. Harn, C.H. Lee, Immunomodulatory glycan LNFPIII alleviates hepatosteatosis and insulin resistance through direct and indirect control of metabolic pathways, Nature Medicine 18(11) (2012) 1665-72.

[16] I.M. Wolfs, J.L. Stoger, P. Goossens, C. Pottgens, M.J. Gijbels, E. Wijnands, E.P. van der Vorst, P. van Gorp, L. Beckers, D. Engel, E.A. Biessen, G. Kraal, I. van Die, M.M. Donners, M.P. de Winther, Reprogramming macrophages to an anti-inflammatory phenotype by helminth antigens reduces murine atherosclerosis, Faseb J 28(1) (2014) 288-99.

[17] I.B. McInnes, B.P. Leung, M. Harnett, J.A. Gracie, F.Y. Liew, W. Harnett, A novel therapeutic approach targeting articular inflammation using the filarial nematode-derived phosphorylcholine-containing glycoprotein ES-62, J Immunol 171(4) (2003) 2127-33.

[18] D.T. Rodgers, M.A. McGrath, M.A. Pineda, L. Al-Riyami, J. Rzepecka, F. Lumb, W. Harnett, M.M. Harnett, The Parasitic Worm Product ES-62 Targets Myeloid Differentiation Factor 88-Dependent Effector Mechanisms to Suppress Antinuclear Antibody Production and Proteinuria in MRL/lpr Mice, Arthritis Rheumatol 67(4) (2015) 1023-35.
[19] A.J. Melendez, M.M. Harnett, P.N. Pushparaj, W.S. Wong, H.K. Tay, C.P. McSharry, W. Harnett, Inhibition of FcepsilonRI-mediated mast cell responses by ES-62, a product of parasitic filarial nematodes, Nature Medicine 13(11) (2007) 1375-81.
[20] J. Rzepecka, I. Siebeke, J.C. Coltherd, D.E. Kean, C.N. Steiger, L. Al-Riyami, C. McSharry, M.M. Harnett, W. Harnett, The helminth product, ES-62, protects against airway inflammation by resetting the Th cell phenotype, International Journal for Parasitology 43(3-4) (2013) 211-23.
[21] T.R. Aprahamian, X. Zhong, S. Amir, C.J. Binder, L.K. Chiang, L. Al-Riyami, R. Gharakhanian, M.M. Harnett, W. Harnett, I.R. Rifkin, The immunomodulatory parasitic worm product ES-62 reduces lupus-associated accelerated atherosclerosis in a mouse model, International Journal for Parasitology 45(4) (2015) 203-7.
[22] C.A. Egan, K.M. Houston, M.J. Alcocer, A. Solovyova, R. Tate, G. Lochnit, I.B. McInnes, M.M. Harnett, R. Geyer, O. Byron, W. Harnett, Lack of immunological cross-reactivity between parasite-derived and recombinant forms of ES-62, a secreted protein of Acanthocheilonema viteae, Parasitology 132(Pt 2) (2006) 263-74.
[23] W. Harnett, J. Rzepecka, K.M. Houston, How do nematodes transfer phosphorylcholine to carbohydrates?, Trends in Parasitology 26(3) (2010) 114-8.
[24] L. Al-Riyami, M.A. Pineda, J. Rzepecka, J.K. Huggan, A.I. Khalaf, C.J. Suckling, F.J. Scott, D.T. Rodgers, M.M. Harnett, W. Harnett, Designing anti-inflammatory drugs from parasitic worms: a synthetic small molecule analogue of the Acanthocheilonema viteae product ES-62 prevents development of collagen-induced arthritis, Journal of Medicinal Chemistry 56(24) (2013) 9982-10002.
[25] J. Rzepecka, M.A. Pineda, L. Al-Riyami, D.T. Rodgers, J.K. Huggan, F.E. Lumb, A.I. Khalaf, P.J. Meakin, M. Corbet, M.L. Ashford, C.J. Suckling, M.M. Harnett, W. Harnett, Prophylactic and therapeutic treatment with a synthetic analogue of a parasitic worm product prevents experimental arthritis and inhibits IL-1beta production via NRF2-mediated counter-regulation of the inflammasome, Journal of Autoimmunity 60 (2015) 59-73.
[26] J. Rzepecka, M.L. Coates, M. Saggar, L. Al-Riyami, J. Coltherd, H.K. Tay, J.K. Huggan, L. Janicova, A.I. Khalaf, I. Siebeke, C.J. Suckling, M.M. Harnett, W. Harnett, Small molecule analogues of the immunomodulatory parasitic helminth product ES-62 have anti-allergy properties, International Journal for Parasitology 44(9) (2014) 669-74.
[27] J.C. Coltherd, D.T. Rodgers, R.E. Lawrie, L. Al-Riyami, C.J. Suckling, W. Harnett, M.M. Harnett, The parasitic worm-derived immunomodulator, ES-62 and its drug-like small molecule analogues exhibit therapeutic potential in a model of chronic asthma, Scientific Reports 6 (2016) 19224.
[28] D.T. Rodgers, M.A. Pineda, C.J. Suckling, W. Harnett, M.M. Harnett, Drug-like analogues of the parasitic worm-derived immunomodulator ES-62 are therapeutic in the MRL/Lpr model of systemic lupus erythematosus, Lupus 24(13) (2015) 1437-42.
[29] C.J. Suckling, S. Alam, M.A. Olson, K.U. Saikh, M.M. Harnett, W. Harnett, Small Molecule Analogues of the parasitic worm product ES-62 interact with the TIR domain of MyD88 to inhibit pro-inflammatory signalling, Scientific Reports 8(1) (2018) 2123.
[30] I. Jialal, H. Kaur, S. Devaraj, Toll-like receptor status in obesity and metabolic syndrome: a translational perspective, J Clin Endocrinol Metab 99(1) (2014) 39-48.
[31] S. Camandola, M.P. Mattson, Toll-like receptor 4 mediates fat, sugar, and umami taste preference and food intake and body weight regulation, Obesity (Silver Spring) 25(7) (2017) 1237-1245.

[32] M. Spiljar, D. Merkler, M. Trajkovski, The Immune System Bridges the Gut Microbiota with Systemic Energy Homeostasis: Focus on TLRs, Mucosal Barrier, and SCFAs, Frontiers in Immunology 8 (2017) 1353.
[33] M.A. Pineda, M.A. McGrath, P.C. Smith, L. Al-Riyami, J. Rzepecka, J.A. Gracie, W. Harnett, M.M. Harnett, The parasitic helminth product ES-62 suppresses pathogenesis in collagen-induced arthritis by targeting the interleukin-17-producing cellular network at multiple sites, Arthritis and Rheumatism 64(10) (2012) 3168-78.
[34] J. Doonan, A. Tarafdar, M.A. Pineda, F.E. Lumb, J. Crowe, A.M. Khan, P.A. Hoskisson, M.M. Harnett, W. Harnett, The parasitic worm product ES-62 normalises the gut microbiota bone marrow axis in inflammatory arthritis, Nature Communications 10(1) (2019) 1554.
[35] B. Guigas, A.B. Molofsky, A worm of one's own: how helminths modulate host adipose tissue function and metabolism, Trends in Parasitology 31(9) (2015) 435-41.
[36] C.W. Liew, J. Boucher, J.K. Cheong, C. Vernochet, H.J. Koh, C. Mallol, K. Townsend, D. Langin, D. Kawamori, J. Hu, Y.H. Tseng, M.K. Hellerstein, S.R. Farmer, L. Goodyear, A. Doria, M. Bluher, S.I. Hsu, R.N. Kulkarni, Ablation of TRIP-Br2, a regulator of fat lipolysis, thermogenesis and oxidative metabolism, prevents diet-induced obesity and insulin resistance, Nature Medicine 19(2) (2013) 217-26.
[37] G.M. Kowalski, M.J. Kraakman, S.A. Mason, A.J. Murphy, C.R. Bruce, Resolution of glucose intolerance in long-term high-fat, high-sucrose-fed mice, J Endocrinol 233(3) (2017) 269-279.
[38] D.L. Tahapary, K. de Ruiter, I. Martin, E.A.T. Brienen, L. van Lieshout, C.M. Cobbaert, P. Soewondo, Y. Djuardi, A.E. Wiria, J.J. Houwing-Duistermaat, E. Sartono, J.W.A. Smit, M. Yazdanbakhsh, T. Supali, Effect of Anthelmintic Treatment on Insulin Resistance: A Cluster-Randomized, Placebo-Controlled Trial in Indonesia, Clin Infect Dis 65(5) (2017) 764-771.
[39] M.A. Pineda, F. Lumb, M.M. Harnett, W. Harnett, ES-62, a therapeutic anti-inflammatory agent evolved by the filarial nematode Acanthocheilonema viteae, Molecular and Biochemical Parasitology 194(1-2) (2014) 1-8.
[40] J. Crowe, F.E. Lumb, J. Doonan, M. Broussard, A. Tarafdar, M.A. Pineda, C. Landabaso, L. Mulvey, P.A. Hoskisson, S.A. Babayan, C. Selman, W. Harnett, M.M. Harnett, Parasitic worm-derived ES-62 promotes health- and life-span in high calorie diet-fed mice BioRxiv (2019) doi.10.1101/622753.
[41] C.W. Su, C.Y. Chen, Y. Li, S.R. Long, W. Massey, D.V. Kumar, W.A. Walker, H.N. Shi, Helminth infection protects against high fat diet-induced obesity via induction of alternatively activated macrophages, Scientific Reports 8(1) (2018) 4607.
[42] F. Pace, B.M. Carvalho, T.M. Zanotto, A. Santos, D. Guadagnini, K.L.C. Silva, M.C.S. Mendes, G.Z. Rocha, S.M. Alegretti, G.A. Santos, R.R. Catharino, R. Paroni, F. Folli, M.J.A. Saad, Helminth infection in mice improves insulin sensitivity via modulation of gut microbiota and fatty acid metabolism, Pharmacological Research : the official journal of the Italian Pharmacological Society 132 (2018) 33-46.

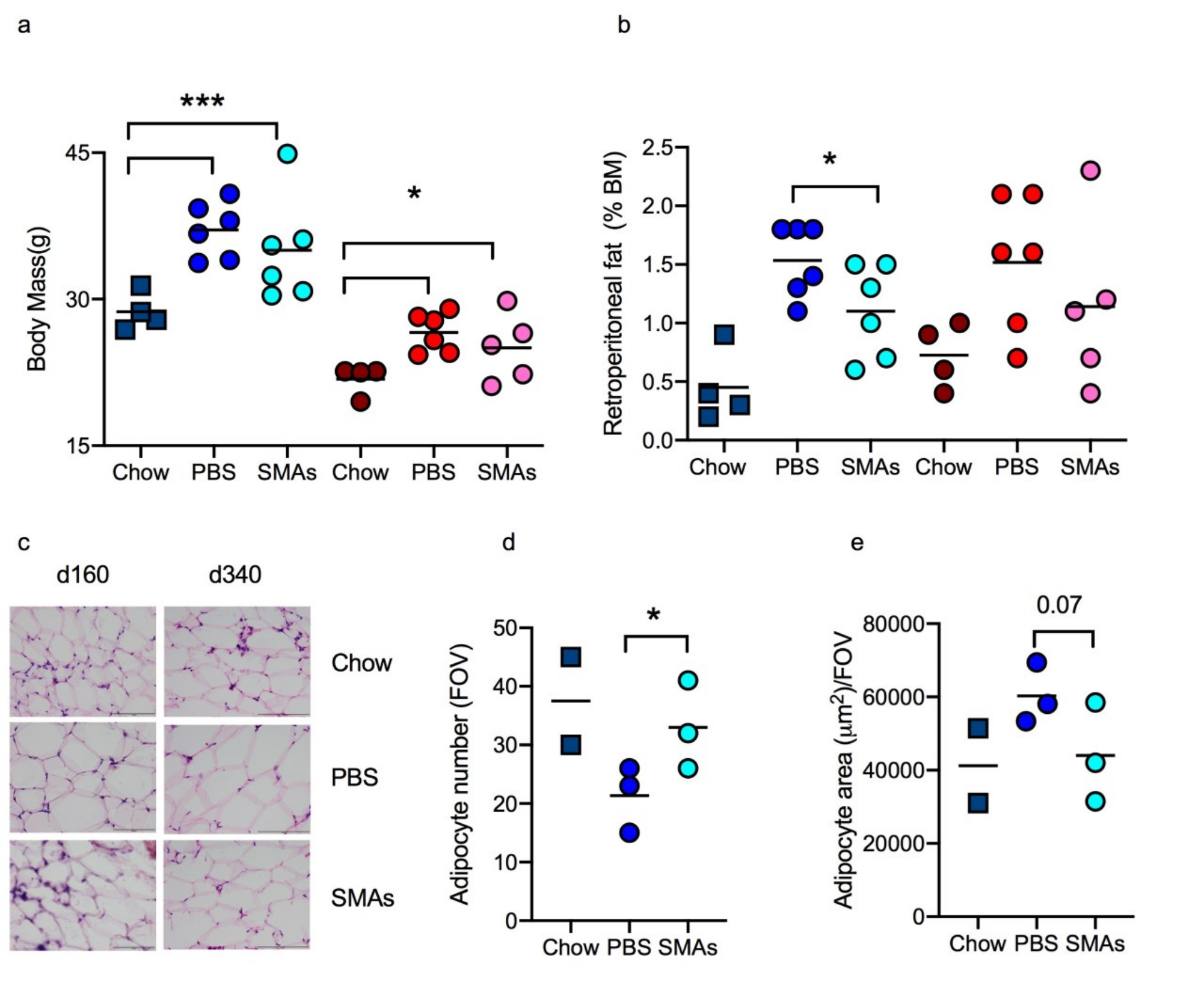
a
***
*
45
30
15
Body Mass(g)
Chow
PBS
SMAs
Chow
PBS
SMAs
b
*
2.5
2.0
1.5
1.0
0.5
0.0
Retroperitoneal fat (% BM)
Chow
PBS
SMAs
Chow
PBS
SMAs
c
d160
d340
Chow
PBS
SMAs
d
*
50
40
30
20
10
0
Adipocyte number (FOV)
Chow
PBS
SMAs
e
0.07
80000
60000
40000
20000
0
Adipocyte area (μm²)/FOV
Chow
PBS
SMAs

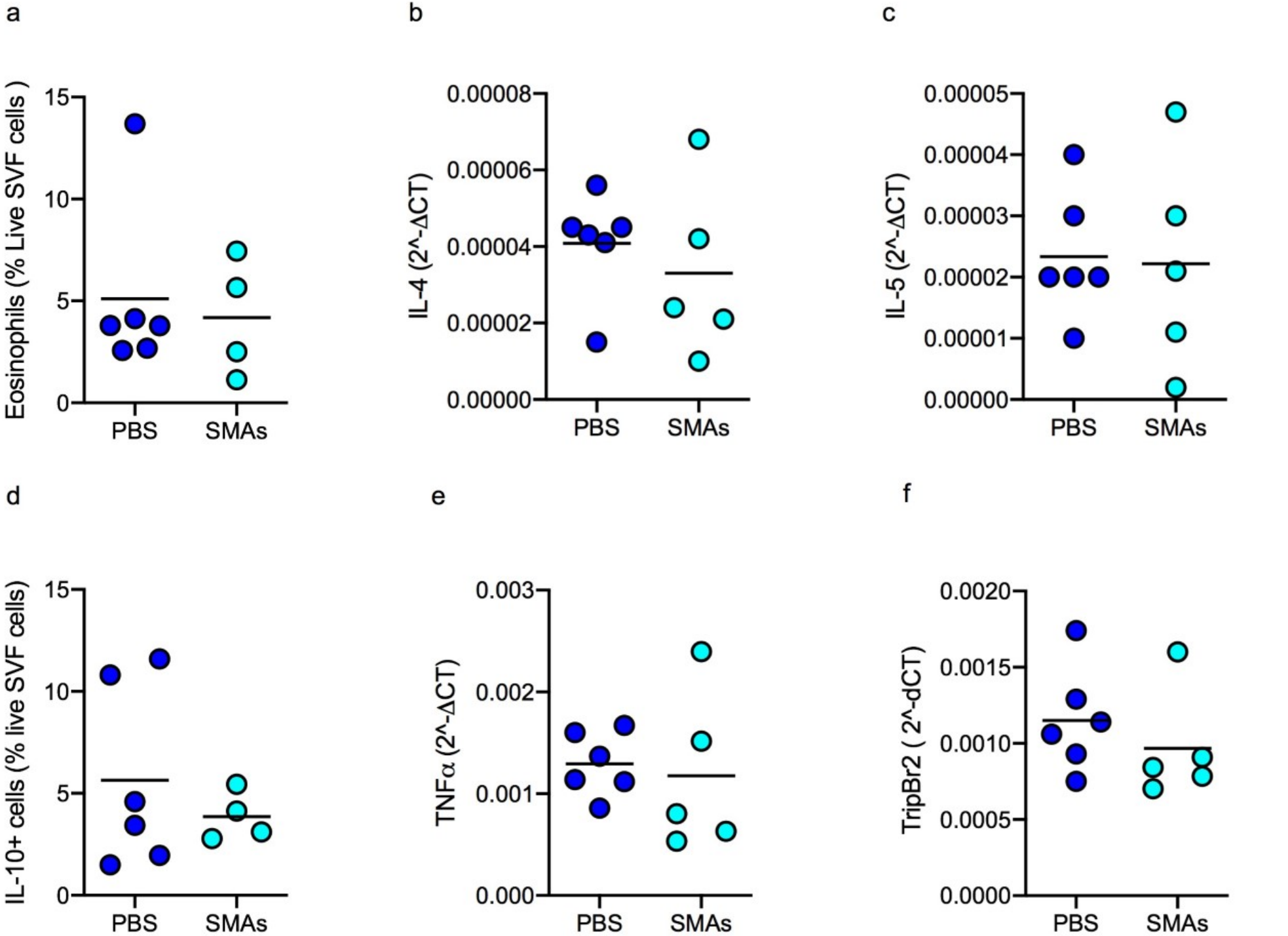
a
Eosinophils (% Live SVF cells)
15
10
5
0
PBS
SMAs
b
IL-4 (2^-ΔCT)
0.00008
0.00006
0.00004
0.00002
0.00000
PBS
SMAs
c
IL-5 (2^-ΔCT)
0.00005
0.00004
0.00003
0.00002
0.00001
0.00000
PBS
SMAs
d
IL-10+ cells (% live SVF cells)
15
10
5
0
PBS
SMAs
e
TNFα (2^-ΔCT)
0.003
0.002
0.001
0.000
PBS
SMAs
f
TripBr2 (2^-dCT)
0.0020
0.0015
0.0010
0.0005
0.0000
PBS
SMAs

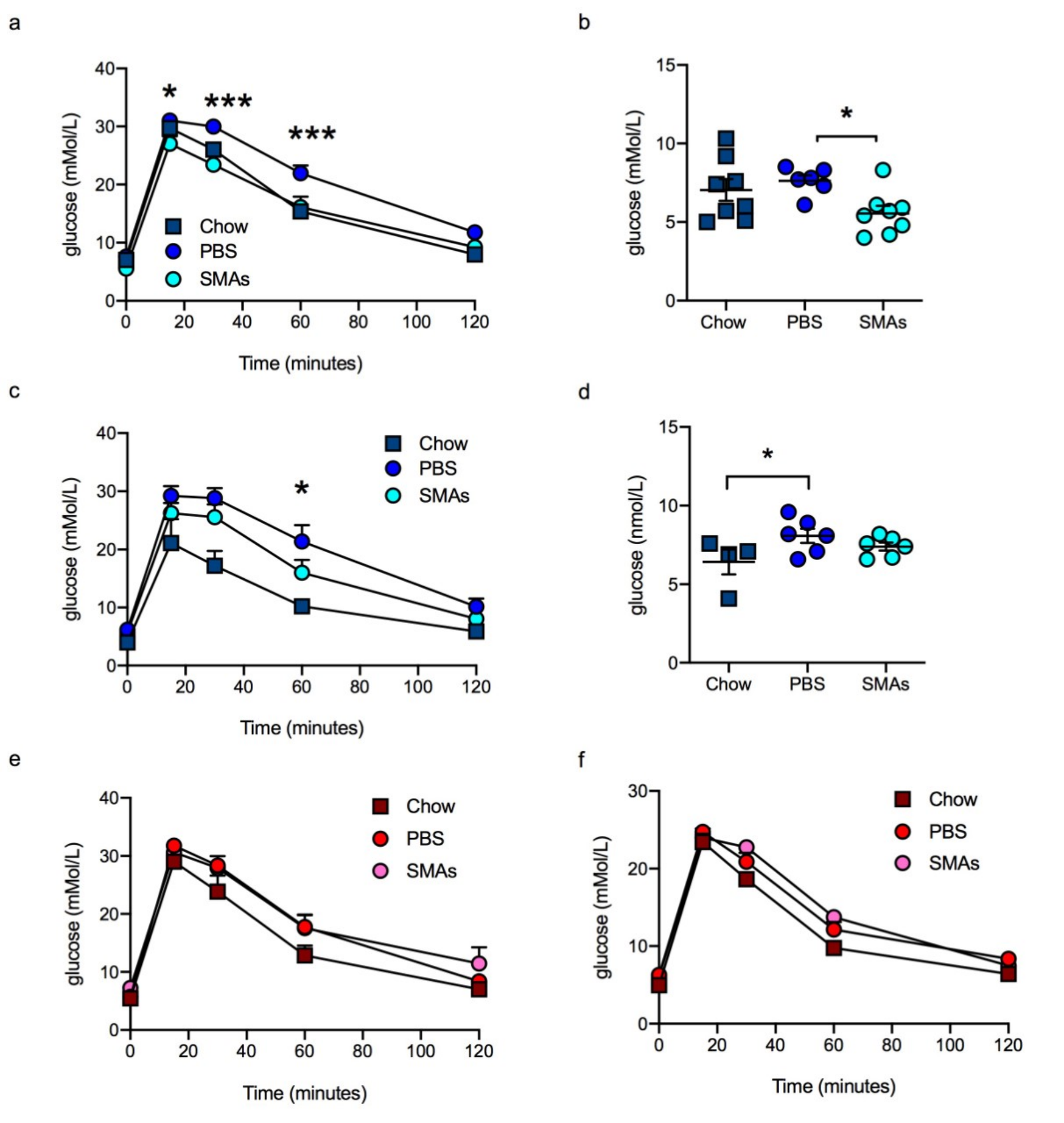
a
b
c
d
e
f
glucose (mMol/L)
Time (minutes)
Chow
PBS
SMAs
glucose (nmol/L)
*
***

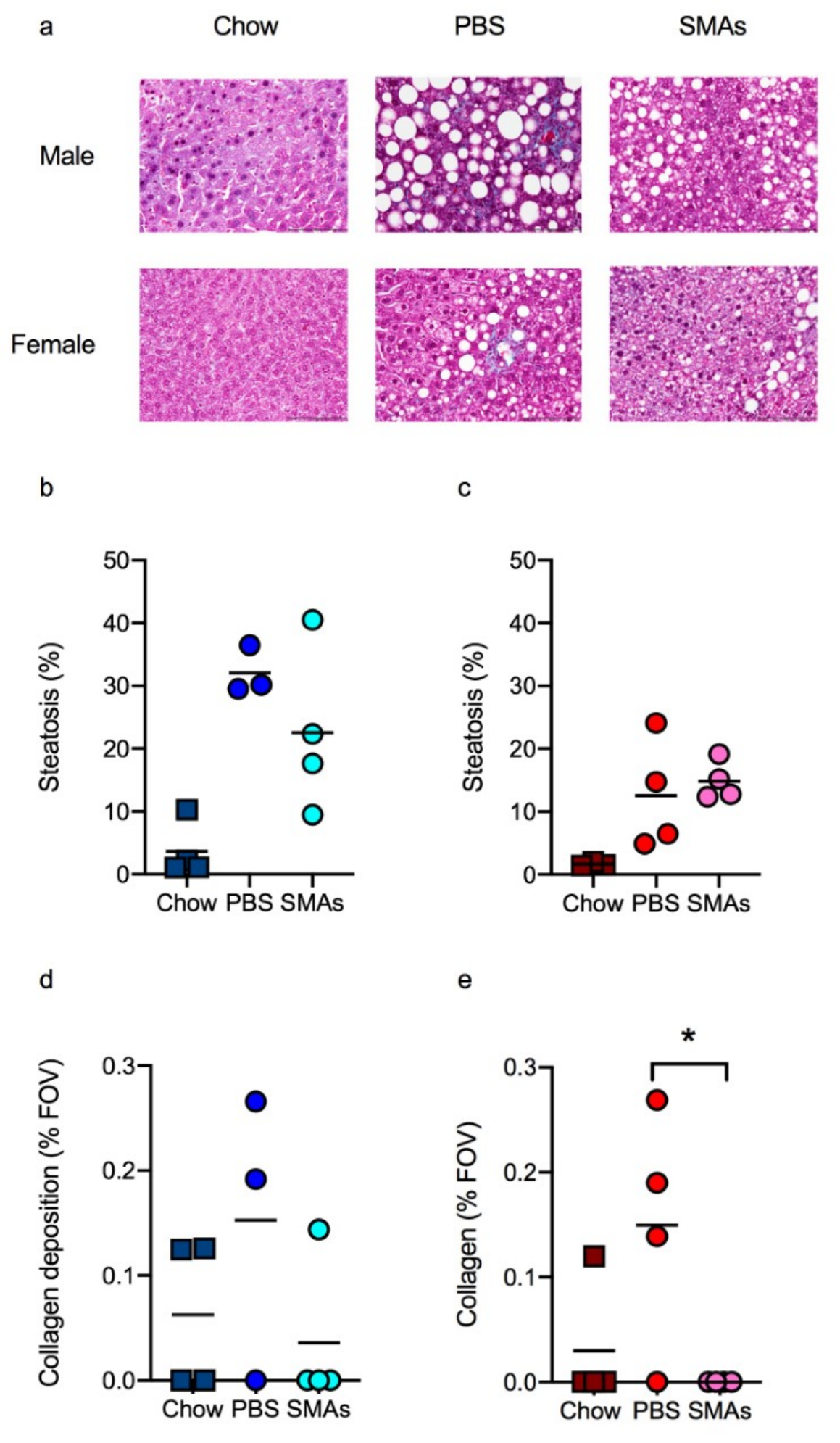
a
Chow
PBS
SMAs
Male
Female
b
Steatosis (%)
50
40
30
20
10
0
Chow PBS SMAs
c
Steatosis (%)
50
40
30
20
10
0
Chow PBS SMAs
d
Collagen deposition (% FOV)
0.3
0.2
0.1
0.0
Chow PBS SMAs
e
*
Collagen (% FOV)
0.3
0.2
0.1
0.0
Chow PBS SMAs

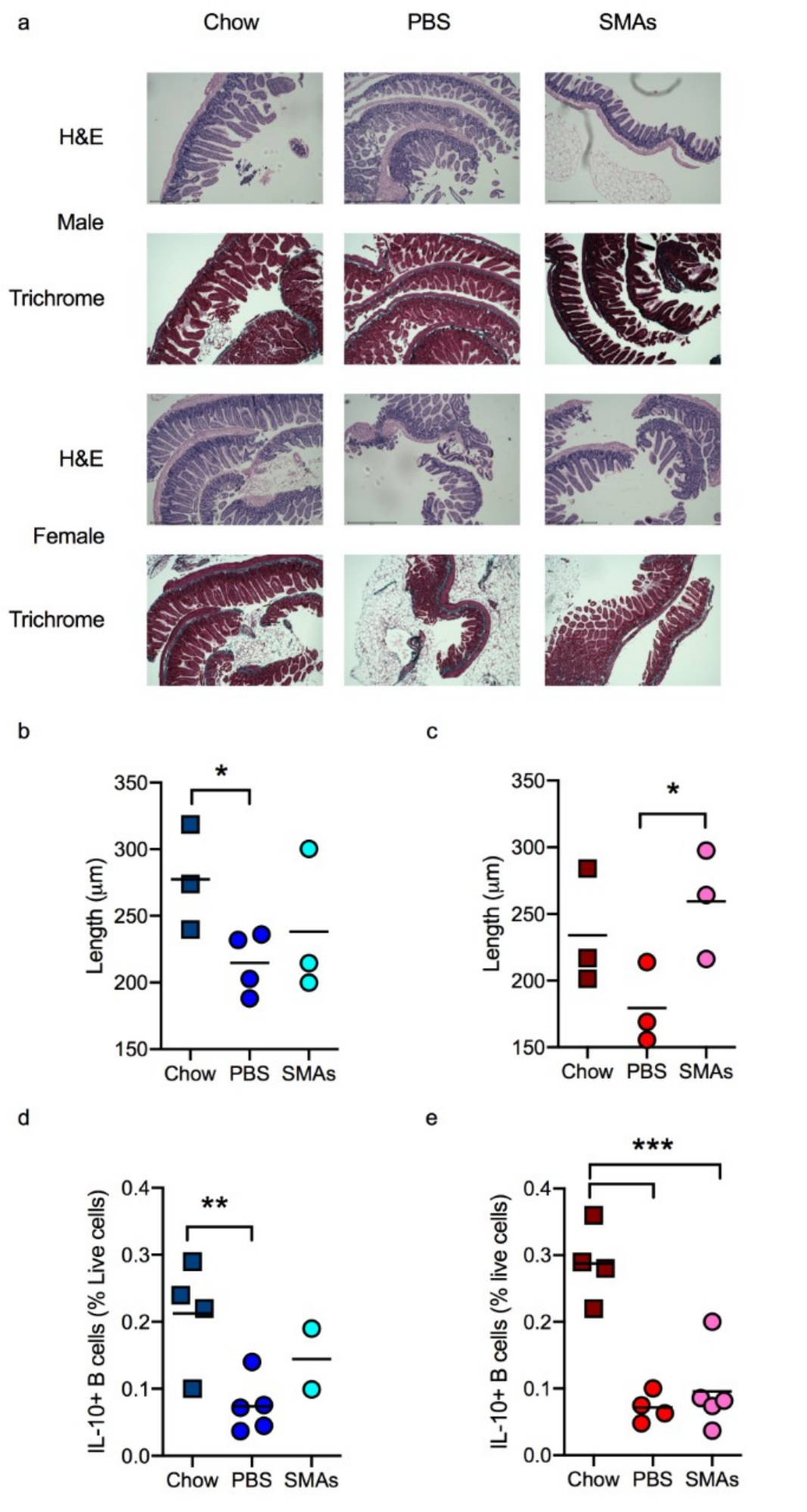
a
Chow
PBS
SMAs
H&E
Male
Trichrome
H&E
Female
Trichrome
b
Length (µm)
350
300
250
200
150
*
Chow
PBS
SMAs
c
Length (µm)
350
300
250
200
150
*
Chow
PBS
SMAs
d
IL-10+ B cells (% Live cells)
0.4
0.3
0.2
0.1
0.0
**
Chow
PBS
SMAs
e
IL-10+ B cells (% live cells)
0.4
0.3
0.2
0.1
0.0
***
Chow
PBS
SMAs

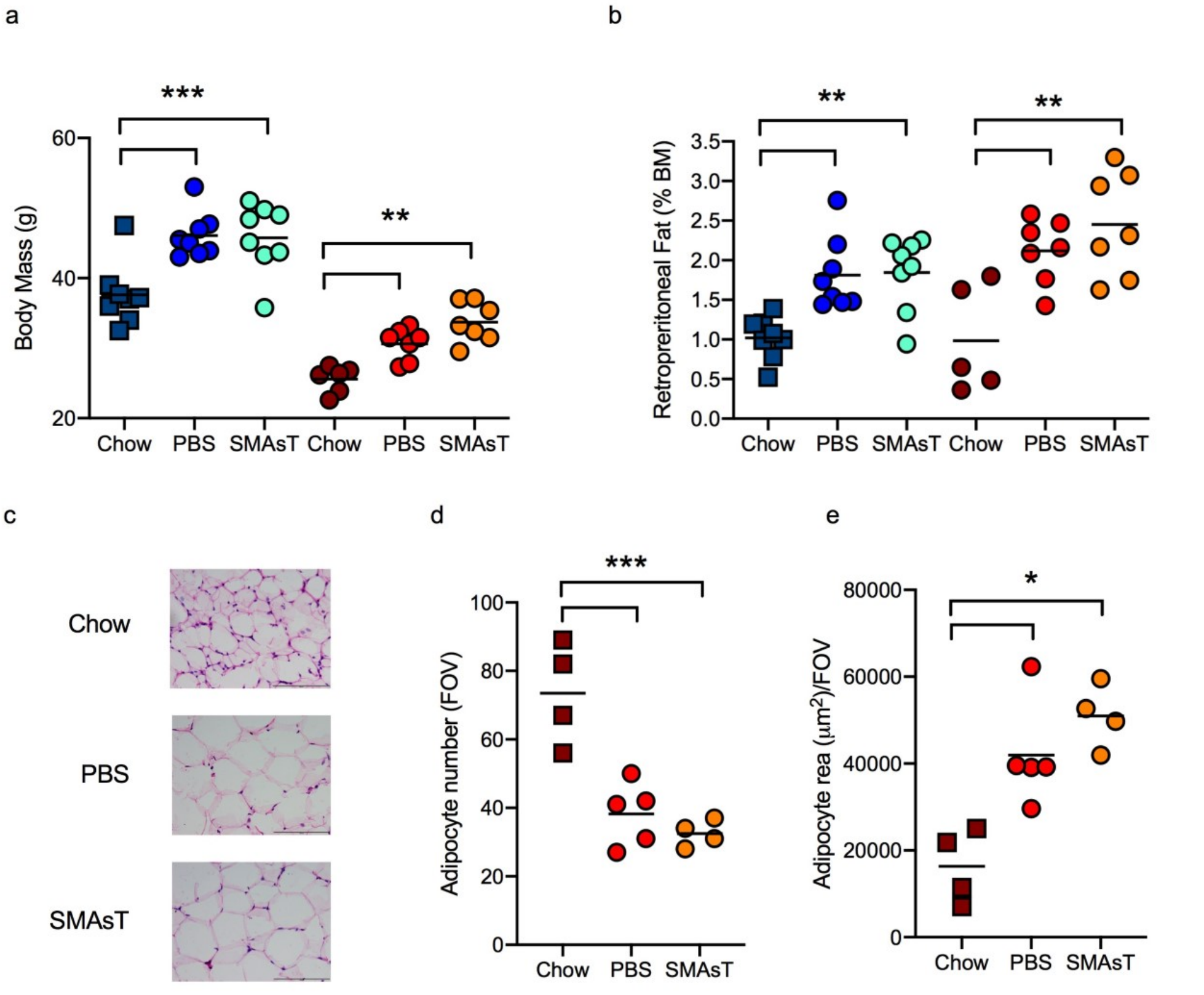
a
***
**
60
40
20
Body Mass (g)
Chow
PBS
SMAsT
Chow
PBS
SMAsT
b
**
**
3.5
3.0
2.5
2.0
1.5
1.0
0.5
0.0
Retropreritoneal Fat (% BM)
Chow
PBS
SMAsT
Chow
PBS
SMAsT
c
Chow
PBS
SMAsT
d
***
100
80
60
40
20
0
Adipocyte number (FOV)
Chow
PBS
SMAsT
e
*
80000
60000
40000
20000
0
Adipocyte rea (μm²)/FOV
Chow
PBS
SMAsT

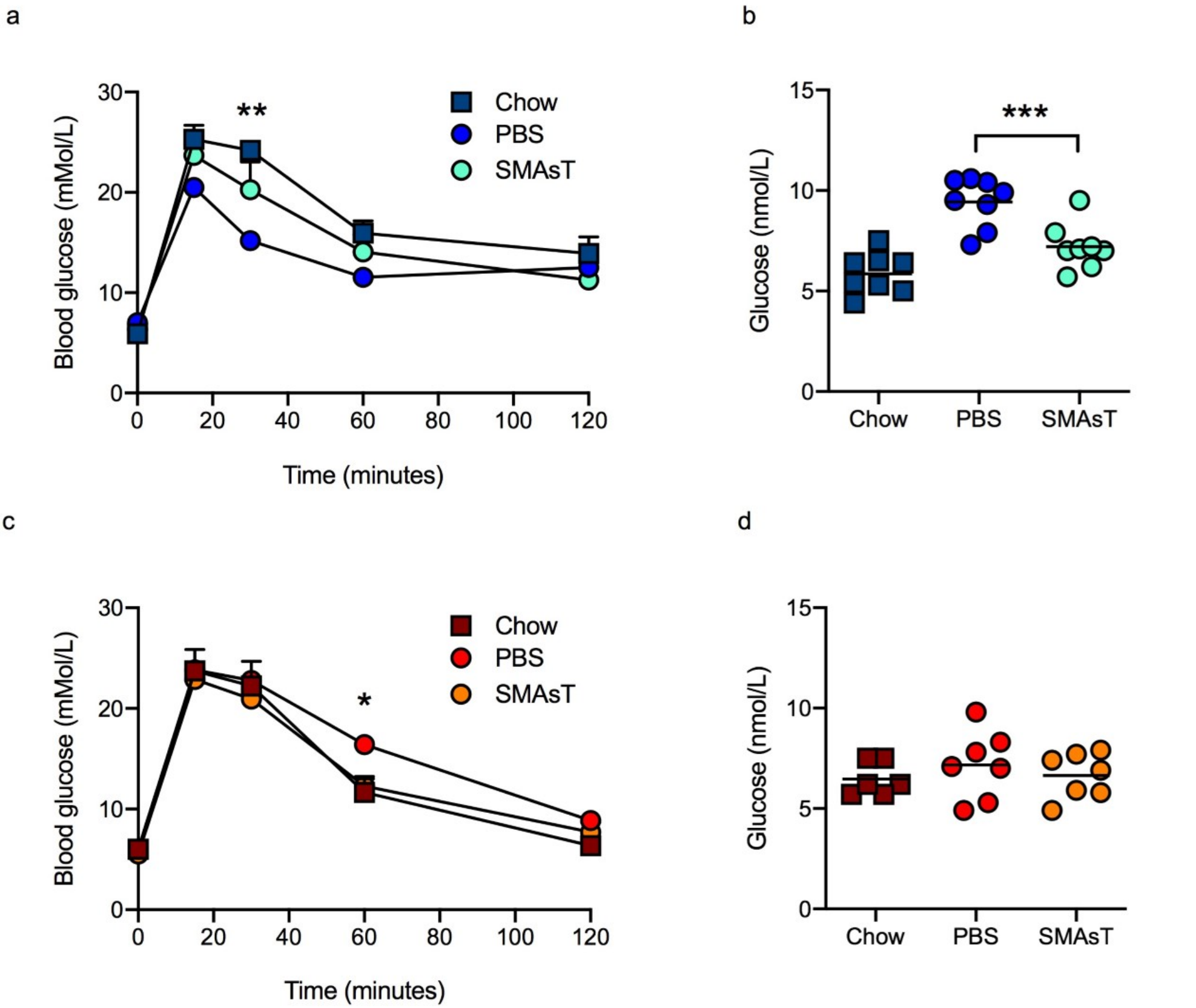
a
b
c
d
Blood glucose (mMol/L)
Time (minutes)
Chow
PBS
SMAsT
**
Glucose (nmol/L)
***
*
0
10
20
30
0
20
40
60
80
100
120
5
15

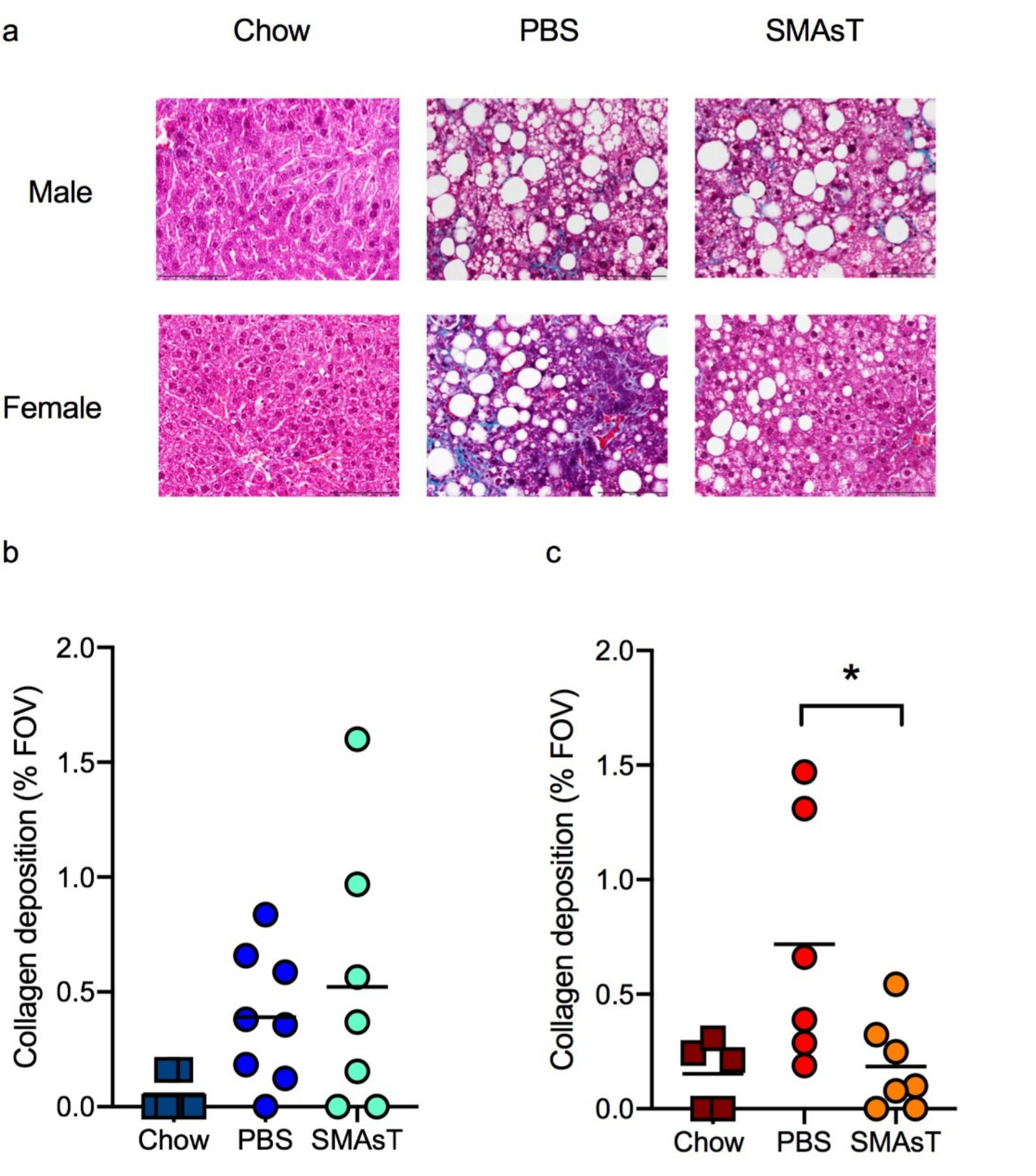
a
Chow
PBS
SMAsT
Male
Female
b
c
Collagen deposition (% FOV)
2.0
1.5
1.0
0.5
0.0
Chow
PBS
SMAsT
*

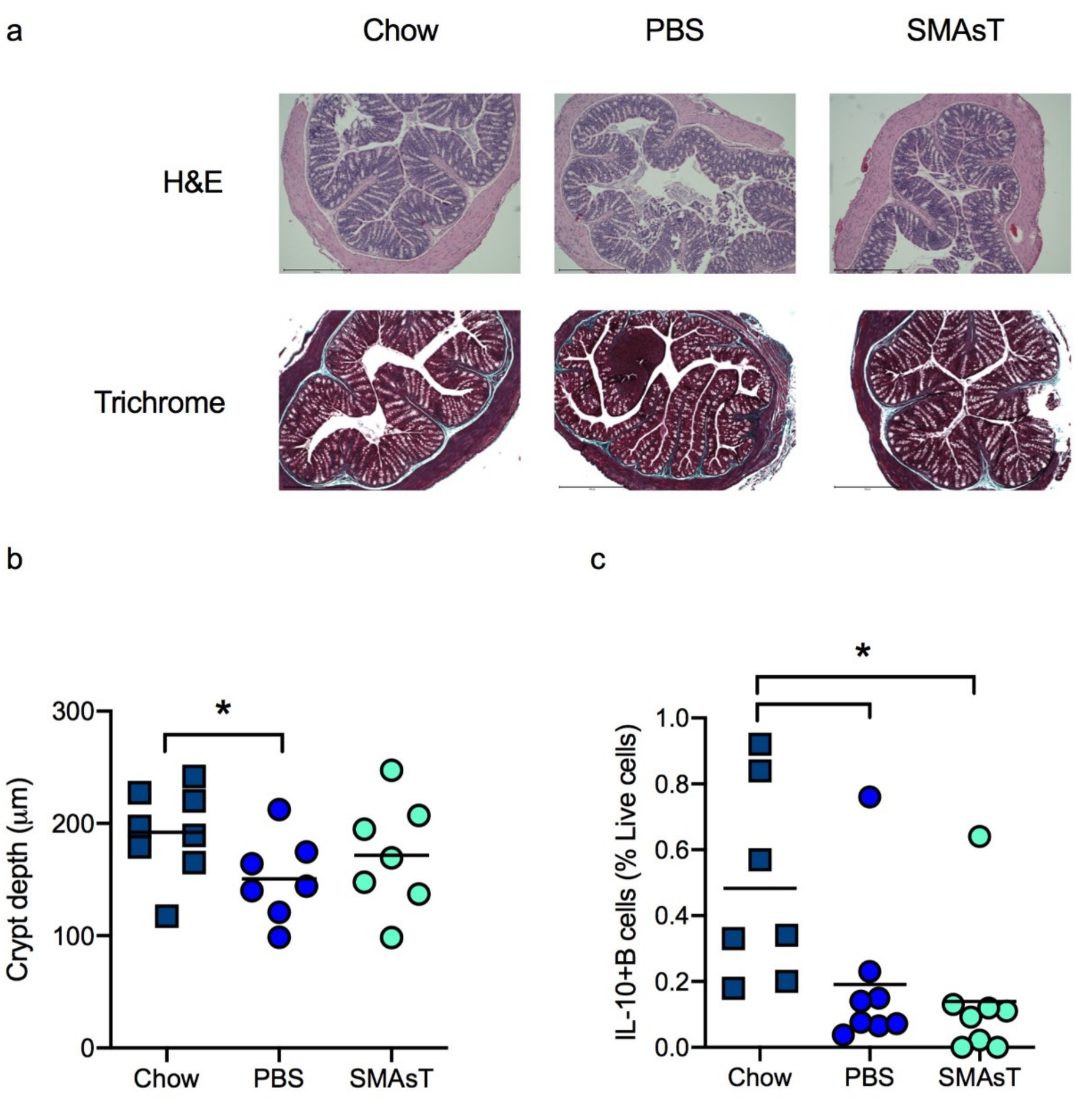
a
Chow
PBS
SMAsT
H&E
Trichrome
b
Crypt depth (µm)
300
200
100
0
*
Chow
PBS
SMAsT
c
IL-10+B cells (% Live cells)
1.0
0.8
0.6
0.4
0.2
0.0
*
Chow
PBS
SMAsT